

# Optimum Signal-to-noise Ratio Performance of Electron Multiplying Charge Coupled Devices

Wen W. Zhang, Qian Chen

**Abstract**—Electron multiplying charge coupled devices (EMCCDs) have revolutionized the world of low light imaging by introducing on-chip multiplication gain based on the impact ionization effect in the silicon. They combine the sub-electron readout noise with high frame rates. Signal-to-noise Ratio (SNR) is an important performance parameter for low-light-level imaging systems. This work investigates the SNR performance of an EMCCD operated in Non-inverted Mode (NIMO) and Inverted Mode (IMO). The theory of noise characteristics and operation modes is presented. The results show that the SNR of is determined by dark current and clock induced charge at high gain level. The optimum SNR performance is provided by an EMCCD operated in NIMO in short exposure and strong cooling applications. In contrast, an IMO EMCCD is preferable.

**Keywords**—electron multiplying charge coupled devices, noise characteristics, operation modes, signal-to-noise ratio performance

## I. INTRODUCTION

ELECTRON multiplying charge coupled devices (EMCCDs) were first introduced to the digital imaging world by E2V Technologies in 2001. They combine the single photon detection sensitivity of an ICCD or an EBCCD with the inherent advantages of the CCD. EMCCDs have long lifetime, small volume, low consume, high spatial resolution and quantum efficiency but without cross-talk, chicken-wire, scintillation, halo effects and the reduced QE. All of these advantages are attributed to the unique all-solid-state electron multiplying structure built into the silicon, which amplify the signal above readout noise floor in charge domain. This allows the EMCCD to run at much faster readout speeds while retaining an excellent imaging quality. EMCCD cameras have proven to be powerful tools and are consequently used in a wide range of fields such as engineering research, biological sciences, astronomical and photometry applications, as in [1]–[3].

W. W. Zhang is with the College of Electrical Engineering and Optoelectronic Technology, Nanjing University of Science & Technology, Nanjing 210094 China (corresponding author to provide phone: 86-25-84315869; fax: 86-25-84303031; e-mail: zhangwenwen1205@hotmail.com).

Q. Chen, is now with the College of Electrical Engineering and Optoelectronic Technology, Nanjing University of Science & Technology, Nanjing 210094 China (e-mail: chenq@mail.njust.edu.cn).

Signal-to-noise ratio (SNR) performance is a key parameter for low-light-level imaging systems. It determines the limit resolution capability. Therefore, the higher the SNR, the better the ability of the system to resolve objects under photon starved conditions, as in [4]. The purpose of this paper is to compare the noise characteristics in different operation modes and determine the optimum SNR performance of the EMCCD. The structure and principle of operation of the EMCCD is well known [2,3] and so only an overview will be given in Section . EMCCDs have two operation modes: Non-inverted Mode Operation (NIMO) and Inverted Mode Operation (IMO). Section describes noise characteristics of the EMCCD in different operation modes. Section compares the SNR variations for both operation modes and concludes the optimum SNR performance of the EMCCD.

## II. THE PRINCIPLE OF EMCCD OPERATION

A frame transfer EMCCD usually consists of five components: image section, storage section, readout register, multiplying register and on-chip charge to voltage converter. Except the image region, other parts are protected from light by an aluminium mask, as shown in Fig. 1.

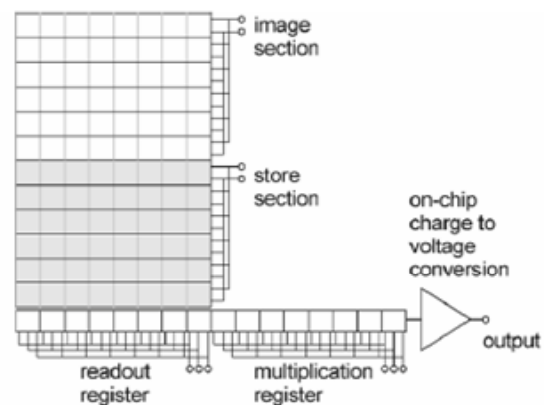


Fig.1 Schematic diagram of an EMCCD

During integration time, the image section is exposed to light and an image is captured. This image is then automatically shifted downwards to storage area which is always identical in size to the image area and then read out. While the image is being read out, the image section is again exposed and the next image is acquired. The aluminium mask therefore acts like an electronic shutter. Then the charge is shifted out through the readout register and into the multiplication register, where

amplification occurs by harnessing a process known as impact ionization, as in [5].

Each element of electron multiplying register is composed of four gates, as shown in Fig. 2. Two of the gates ( $\phi 1$  and  $\phi 3$ ) are clocked with normal amplitude drive pulses ( $\sim 10$  Volts) and can use the same pulses as those applied to two phases of the readout register. The pulses applied to  $\phi 2$  of the multiplication element have higher amplitude, typically 40~45 Volts. A gate is placed prior to  $\phi 2$ , which is held at a low DC level. The potential difference between  $\phi_{dc}$  and the high level of  $\phi 2$  can be set sufficiently high so that signal electrons can undergo impact ionization processes as they are transferred from  $\phi 1$  to  $\phi 2$  during the normal clocking sequence. Thus the number of electrons in the charge packet increases as it passes through a multiplication element, as in [6], [7]. Although the multiplication gain per transfer is very low, only around  $X 1.01 \sim X 1.015$ . The total gain of the cascaded multiplication is quite significant. For example, with  $X 1.015$  multiplication per transfer over 591 transfers (in the case of the CCD65), a gain of 1.015 to the power of 591, equaling  $X 6630$ , is achieved, as in [8].

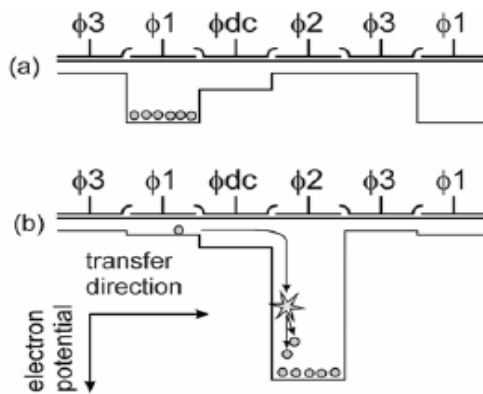


Fig.2 Charge transfer through a multiplication element

### III. NOISE CHARACTERISTICS

In an EMCCD, noise components consist of photon shot noise, dark current noise, clock induced charge noise, noise factor and readout noise.

#### A. Photon Shot Noise

Photon shot noise is due to the particle nature of photons and results from the inherent statistical variation in the arrival rate of photons incident on the CCD. It is a fundamental property of the quantum nature of light and unavoidable in imaging systems. Photon shot noise constitutes the theoretical noise limitation of any low-light-level imaging system, as in [9]. The interval between photon arrivals is governed by Poisson statistics, and therefore, the photon shot noise is equivalent to the square-root of the signal:

$$N_p = \sqrt{S} = \sqrt{P\eta t} \quad (1)$$

where  $S$  is detected signal,  $P$  is mean incident photon flux,  $\eta$  is quantum efficiency of the EMCCD,  $t$  is integration time.

#### B. Dark Current Noise

Dark current is caused by thermally generated electrons in the silicon substrate, which is independent of photon-induced signal, but highly dependent on device temperature. Generally three different dark current components contribute to total dark current in an EMCCD: the dark current generated at the silicon surface (surface dark current, caused by Si-SiO<sub>2</sub> interface states), the dark current generated in the depletion region, and the diffusion dark current generated in the field-free region. The latter two types are usually called bulk dark current.

For an EMCCD operated in NIMO (also called Normal Mode), clocks applied to image section is positive. Signal channel and Si-SiO<sub>2</sub> interface states are depleted of free carriers thus maximizing dark current generation. In NIMO, dark current is determined by the density of Si-SiO<sub>2</sub> interface states. Therefore, the surface dark current is dominant, being typically two orders greater than the bulk dark current, as shown in Fig.3.

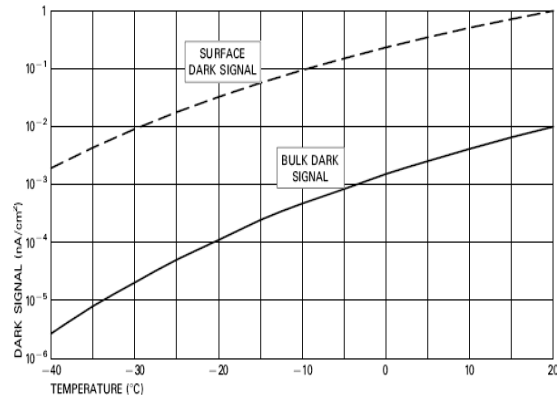


Fig.3 Surface and bulk dark current versus temperature

The surface dark current in nA/cm<sup>2</sup> given by, as in [10]:

$$I_d \approx I_s = 122T^3 \exp(-6400/T) \quad (2)$$

where  $I_d$  is the total dark current of the EMCCD,  $T$  is the device operation temperature in Kelvin.

For an EMCCD operated in IMO (also called Multi Pinned Phase, MPP), clocks applied to image section is negative. Signal channel is inverted and surface potential beneath each phase is pinned to substrate potential. Biasing the array clocks in this manner causes holes from the p+ channel stops to migrate and populate the Si-SiO<sub>2</sub> interface states. Thermally generated electrons can't hop from the valance band to the conduction band through Si-SiO<sub>2</sub> interface states. Hence the surface dark current generation is almost completely suppressed in IMO, as in [11]. Reference [10] shows that the depletion dark current dominates at the temperature below  $\sim 240$ K. It is described by:

$$I_d \approx I_b = CT^n \exp(-E_g / 2kT) \quad (3)$$

where  $I_b$  is the bulk dark current,  $C$  is constant,  $n \in [1, 3]$ ,  $E_g$  is the band gap energy of silicon,  $k$  is Boltzmann's constant.

If the temperature is above ~300K, the diffusion dark current forms dominant contribution, which can be given by:

$$I_d \approx I_b = CT^n \exp(-E_g / kT) \quad (4)$$

If the temperature is between 240K~300K, both depletion dark current and diffusion dark current are important. To describe the temperature variation of dark current in this intermediate region, E2V technologies scaling relationship was developed:

$$I_d \approx I_b = 3.3 \times 10^6 T^2 \exp(-9080/T) \quad (5)$$

In similarity to photon shot noise, dark current noise follows a Poisson relationship to dark current, and is equivalent to the square-root of the number of thermal electrons generated within the image integration time:

$$N_d = \sqrt{I_d t} \quad (6)$$

Cooling the EMCCD reduces the dark current dramatically, and in practice, high performance cameras are usually cooled to a temperature at which dark current is negligible over a typical integration interval.

C. Clock Induced Charge Noise

When a CCD is driven into inversion, holes from the channel stops migrate and collect beneath the gate pinning the surface substrate potential. Some of the holes become trapped at the Si-SiO<sub>2</sub> interface states. When the clock is switched out of inversion to transfer charge the trapped holes are accelerated out of the Si-SiO<sub>2</sub> interface states. Some holes are released with sufficient energy to create electron-hole pairs by impact ionization. These spurious electrons are collected in the nearest potential well and called Clock Induced Charge (CIC) or Spurious Charge. CIC events are generated in every CCD but are normally completely buried in the readout noise, thus ignored. However, for the EMCCD at high gain, even individual electrons can be seen as sharp spikes in the image. Since the dark current noise is minimized to negligible level through effective cooling, clock induced charge becomes the main noise source.

For an EMCCD operated in NIMO, Si-SiO<sub>2</sub> interface states are holes-depleted and a typical CIC value of approximately 3×10<sup>-6</sup>e<sup>-</sup>/pixel/transfer for typical clock amplitudes. For an EMCCD operated in IMO, Si-SiO<sub>2</sub> interface states are completely populated with holes and the CIC increases to approximately 1×10<sup>-4</sup>e<sup>-</sup>/pixel/transfer at normal clock amplitudes, as show in Fig. 4. CIC increases exponentially with clock amplitudes and rising edge speeds. It also increases linearly on the number of parallel transfers that take place. CIC is integration time and temperature independent. The noise caused by CIC acts as shot noise, which is given by:

$$N_c = \sqrt{mc} \quad (7)$$

where *m* is the total number of parallel transfers, *c* is typical CIC value in different operation modes.

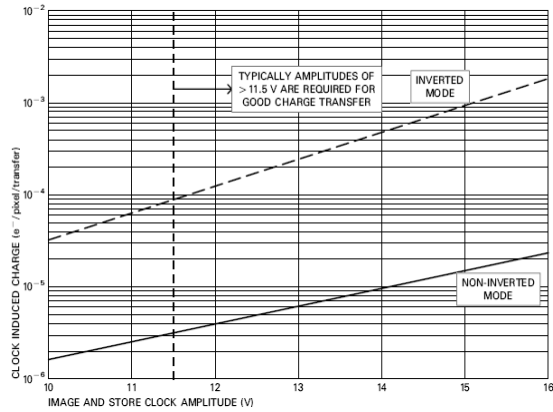


Fig.4 Typical clock induce charge for operation in IMO and NIMO

D. Noise Factor

Due to the probabilistic nature of the impact ionization process utilized in the EMCCD, a statistical variation occurs in the on-chip multiplication gain. The uncertainty in the gain produced introduces an additional system noise component, which is evaluated quantitatively as the noise factor *F*. It can be defined by the following, as in [12]:

$$F^2 = \frac{\sigma_{out}^2}{G^2 \sigma_{in}^2} \quad (8)$$

where *G* is total multiplication gain,  $\sigma_{in}^2$  and  $\sigma_{out}^2$  are the variances of the input and output signals respectively. If the gain process is ideal and adds no noise then noise factor will be unity. However, the stochastic multiplication process and any loss mechanisms introduce noise. It has been proved by theoretical and experimental analysis that noise factor of an EMCCD approaches to a value of  $\sqrt{2}$  at high gain.

E. Readout Noise

Readout noise is a combination of system noise components inherent to the process of converting signal charge carriers into a voltage signal for quantification, and the subsequent electronic circuitry and analog-to-digital (A/D) conversion. The major contribution to readout noise usually originates with the on-chip preamplifier, and this noise is added uniformly to each image pixel. Certain types of noise in the output amplifier are frequency dependent and the required readout rate or frame rate partially determine the readout noise specification and its practical effect on overall SNR level, as in [13]. For conventional CCDs, readout noise becomes dominant noise at high frame rates. High performance camera systems always utilize design enhancements (e.g. Correlated Double Sampling Technique) that dramatically reduce the significance of readout noise. In an EMCCD, effective readout noise is reduced to sub-electron level when multiplication gain is high enough, therefore eliminating this primary contribution to the instrumental detection limit.

F. Total Noise

Due to the architecture of the EMCCD, noise sources entering the multiplication register will be multiplied up along with signal charge, such as photon shot noise, dark current noise and clock induced charge. Thus, total noise generated by an EMCCD is given by:

$$N_{tot} = \sqrt{F^2 G^2 (N_p^2 + N_d^2 + N_c^2) + N_r^2} \quad (9)$$

where  $N_r$  is readout noise.

IV. OPTIMUM SNR PERFORMANCE & CONCLUSION

From the above noise descriptions, it is apparent that dark current noise is obvious in NIMO and clock induced charge noise is evident in IMO. Here we compare the SNR performance in two different operation modes and determine the optimum SNR of the EMCCD. The SNR of an EMCCD can be expressed as follows:

$$SNR = \frac{S}{N_{tot}} = \frac{P\eta t}{\sqrt{F^2 (P\eta t + I_d t + mc) + \left(\frac{N_r}{G}\right)^2}} \quad (10)$$

Therefore, the SNR in NIMO and IMO is separately given by:

$$SNR_{ni} = \frac{P\eta t}{\sqrt{F^2 (P\eta t + I_s t + mc_{ni}) + \left(\frac{N_r}{G}\right)^2}} \quad (11)$$

$$SNR_i = \frac{P\eta t}{\sqrt{F^2 (P\eta t + I_b t + mc_i) + \left(\frac{N_r}{G}\right)^2}} \quad (12)$$

where  $c_{ni}$  and  $c_i$  are typical CIC values in NIMO and IMO.

A front-illuminated EMCCD was chosen for simulation with following parameters:  $\eta = 50\%$ ,  $N_r = 20 \text{ e}^- \text{ rms}$ ,  $m = 1000$ ,  $c_{ni} = 3 \times 10^{-6} \text{ e}^-/\text{pixel}/\text{transfer}$ ,  $c_i = 1 \times 10^{-4} \text{ e}^-/\text{pixel}/\text{transfer}$ ,  $F = \sqrt{2}$ ,  $G = 1000$ . Firstly, we assume an integration time of 20ms. Fig. 5 and 6 shows the SNR variation as a function of mean incident photon flux in NIMO and IMO when the sensor temperature is 300K and 240K respectively. Comparing Fig. 5 and 6, the SNR performance in IMO always outperforms that in NIMO. However, the SNR difference between NIMO and IMO is small at low temperature, because the dark current noise decreases drastically at 240K and the SNR in NIMO is improved significantly in low-light-level conditions.

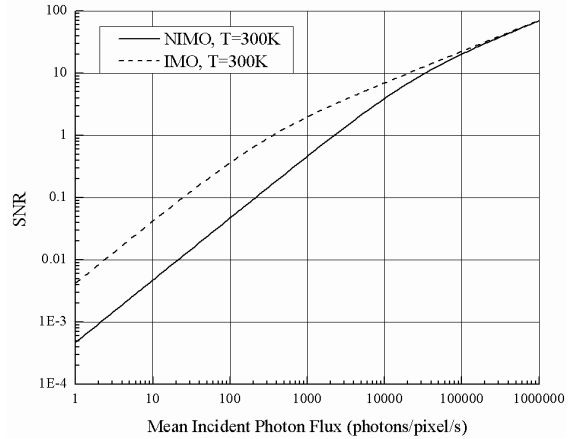


Fig. 5 Variation of the SNR versus signal in NIMO and IMO at 20ms integration time, with high temperature (T=300K).

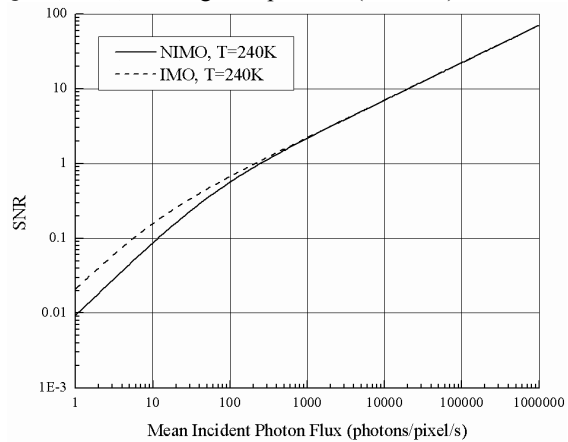


Fig. 6 Variation of the SNR versus signal in NIMO and IMO at 20ms integration time, with low temperature (T=240K).

Secondly, we assume mean incident photon flux arriving at the EMCCD equals 1000 photons/pixel/s. Fig. 7 and 8 shows the SNR variation as a function of integration time in NIMO and IMO when the sensor temperature is 300K and 240K respectively.

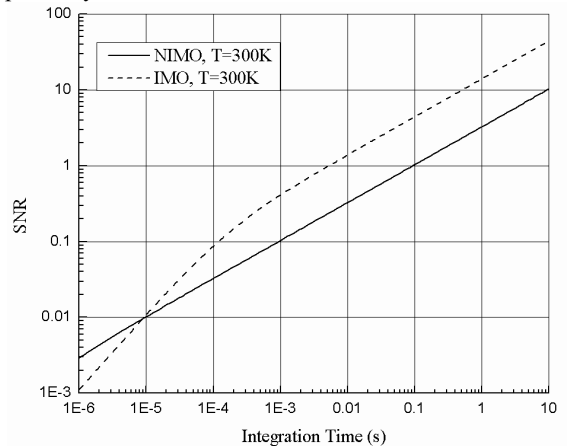


Fig. 7 Variation of the SNR versus integration time in NIMO and IMO at 1000 photons/pixel/s versus integration time in NIMO and IMO at 1000 photons/pixel/s mean incident photon flux, with high temperature (T=300K).

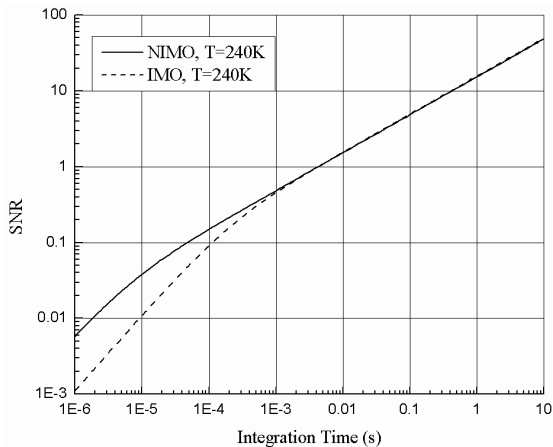


Fig. 8 Variation of the SNR versus integration time in NIMO and IMO at 1000 photons/pixel/s mean incident photon flux, with low temperature ( $T=240\text{K}$ ).

In Fig. 7, for an integration time roughly less than  $10^{-5}$  second, the SNR in NIMO is prior to that in IMO at 300K. Since the photon shot noise and dark current noise are both functions of integration time, they are negligible at very short exposure. CIC noise becomes the dominant noise source and determines the SNR performances. In Fig. 8, the SNR in NIMO is better than that in IMO all the time at 240K. Dark current noise is almost eliminated through sufficient cooling. Due to lower CIC, the EMCCD operated in NIMO provides higher SNR performance. Therefore, we conclude that an EMCCD operated in NIMO offers the optimum SNR performance in short integration time and strong cooling conditions. In contrast, an EMCCD operated in IMO is the optimum choice.

#### REFERENCES

- [1] A. O'Grady, "A comparison of EMCCD, CCD and emerging technologies optimized for low light spectroscopy applications," in *Proc. SPIE Biomedical Vibrational Spectroscopy III: Advances in Research and Industry*, 2006, pp. 60930S-1–60930S-9.
- [2] P. J. Pool, D. G. Morris, D. J. Burt, R. T. Bell, A. D. Holland, *et al.*, "Application of electron multiplying CCD technology in space instrumentation," in *Proc. SPIE Focal Plane Arrays for Space Telescopes II*, 2005, pp. 59020A-1–59020A-6
- [3] N. Smith, C. Coates, A. Giltinan, J. Howard, A. O'Connor, *et al.*, "EMCCD Technology and its Impact on Rapid Low-Light Photometry," in *Proc. SPIE Optical and Infrared Detectors for Astronomy*, 2004, pp. 162–172.
- [4] D. Dussault and P. Hoess, "Noise performance comparison of ICCD with CCD and EMCCD cameras," in *Proc. SPIE Infrared Systems and Photoelectronic Technology*, 2004, pp.195–204.
- [5] C. Coates. (2006, January). EMCCD cameras taking imaging to a new level. *Optics*. [Online]. pp. 29–31. Available: <http://optics.org/cws/article/research/23938>
- [6] M. S. Robbins and B. J. Hadwen, "The Noise Performance of Electron Multiplying Charge Coupled Devices," *IEEE Trans. Electron Devices*, vol. 50, pp. 1227–1232, May. 2003.
- [7] P. A. Jerram, P. J. Pool, D. J. Burt, R. T. Bell and M. S. Robbins, "Electron Multiplying CCDs," in *SNIC Symposium*, 2006, pp. 1–5.
- [8] D. J. Denvir and C. G. Coates, "Electron-multiplying CCD technology: application to ultrasensitive detection of biomolecules," in *Proc. SPIE Biomedical Nanotechnology Architectures and Applications*, 2002, pp. 502–512.
- [9] *E2V Technologies Low-Light Technical Note 2*, E2V Technologies Limited, L3Vision, Chelmsford, 2003.
- [10] *E2V Technologies Low-Light Technical Note 4*, E2V Technologies Limited, L3Vision, Chelmsford, 2004.
- [11] SITe 1024 x 1024 Thermoelectrically Cooled Scientific-Grade CCD, Scientific Imaging Technologies INC., SIA003A, Rockwell, 1995.
- [12] J. Hyncek and T. Nishiwaki, "Excess Noise and Other Important Characteristics of Low Light Level Imaging Using Charge Multiplying CCDs," *IEEE Trans. Electron Devices*, vol. 50, pp. 239–245, Jan. 2003.
- [13] Hamamatsu Learning Center: CCD Noise Sources and Signal-to-Noise Ratio. [Online]. Available: <http://learn.hamamatsu.com/articles/ccdsnr.html>

**Wen W. Zhang** was born in China in 1981. In 2004 she received her bachelor's degree in electronic science and technology from Nanjing University of Science & Technology, China. Now she is taking successive postgraduate and doctoral programs in optical engineering in the same university.

She has authored and co-authored several papers in the field of image processing and signal analysis.

**Qian Chen** was born in China in 1964. In 1996, he received his Ph.D. degree in optical engineering from Nanjing University of Science & Technology, China.

In 1993 he was appointed to Research Fellow working with the City University of Hong Kong collaboration. Since 1995, he has been working for Nanjing University of Science & Technology on the development and application of optoelectronic imaging theory and technology. He is currently a dean of College of Electrical Engineering and Optoelectronic Technology, and an advisor of Ph.D. professor. He has authored and co-authored 80 papers in the field of optoelectronic imaging devices and systems. He has participated in the paper review process for various journals.

Prof. Chen is a member of SPIE. He was awarded chair professor of Cheung Kong Scholars Program in 2005. He was also the winner of National Government Special Allowance and National Outstanding Contribution Medium & Youth Expert.